Synthetic lethal interactions with conditional poly(A) polymerase alleles identify LCP5, a gene involved in 18S rRNA maturation

T. Wiederkehr, R. F. Pretot and L. Minvielle-Sebastia

RNA 1998 4: 1357-1372

RNA (1998), *4*:1357–1372. Cambridge University Press. Printed in the USA.

Synthetic lethal interactions with conditional poly(A) polymerase alleles identify *LCP5*, a gene involved in 18S rRNA maturation

THOMAS WIEDERKEHR, RENÉ F. PRÉTÔT, and LIONEL MINVIELLE-SEBASTIA
Department of Cell Biology, Biozentrum, University of Basel, Klingelbergstrasse 70, CH-4056, Basel, Switzerland

ABSTRACT

To identify new genes involved in 3′-end formation of mRNAs in *Saccharomyces cerevisiae*, we carried out a screen for synthetic lethal mutants with the conditional poly(A) polymerase allele, *pap1-7*. Five independent temperature-sensitive mutations called *lcp1* to *lcp5* (for lethal with conditional *pap1* allele) were isolated. Here, we describe the characterization of the essential gene *LCP5* which codes for a protein with a calculated molecular mass of 40.8 kD. Unexpectedly, we found that mutations in *LCP5* caused defects in pre-ribosomal RNA (pre-rRNA) processing, whereas mRNA 3′-end formation in vitro was comparable to wild-type. Early cleavage steps (denoted A_0 to A_2) that lead to the production of mature 18S rRNA were impaired. In vivo depletion of Lcp5p also inhibited pre-rRNA processing. As a consequence, mutant and depleted cells showed decreased levels of polysomes compared to wild-type cells. Indirect immunofluorescence indicated a predominant localization of Lcp5p in the nucleolus. In addition, antibodies directed against Lcp5p specifically immunoprecipitated the yeast U3 snoRNA snR17, suggesting that the protein is directly involved in pre-rRNA processing.

Keywords: ribosome biogenesis; translation; U3 snoRNP

INTRODUCTION

The poly(A) tail found at the 3′ end of eukaryotic messenger RNAs (mRNAs) is an essential modification that occurs at the posttranscriptional level (for reviews, see Keller, 1995; Manley & Takagaki, 1996; Wahle & Keller, 1996; Colgan & Manley, 1997; Keller & Minvielle-Sebastia, 1997). Besides its probable involvement in nucleocytoplasmic transport and RNA localization, the poly(A) tail plays important roles in mRNA stability and in translation (Gallie, 1991; Gallie & Tanguay, 1994; Caponigro & Parker, 1995; for reviews, see Sachs & Wahle, 1993; Jacobson & Peltz, 1996; Sachs et al., 1997). The function of the poly(A) tail in translation is mediated by Pab1p (Sachs & Davis, 1989; Tarun & Sachs, 1995). Synthetic lethal interaction and coimmunoprecipitation studies showed that the eukaryotic translation initiation factor eIF4G binds Pab1p and that this binding is required to stimulate translation of polyadenylated mRNAs (Tarun & Sachs, 1996; Tarun et al., 1997). Because eIF4G also interacts with the cap-binding protein eIF4E (Haghighat & Sonenberg, 1997), a direct link between the 3′ and the 5′ ends of the mRNA is likely to occur. Consistent with these observations, discrimination against poly(A)-deficient mRNAs was observed during translation when synthesis of ribosomal subunits was impaired (Proweller & Butler, 1997).

Synthetic lethality (Huffacker et al., 1987; Guarente, 1993) has been shown to be an efficient genetic method in the analysis of multisubunit complexes involved in splicing, rRNA processing, or nucleopore assembly (Frank et al., 1992; Venema & Tollervey, 1996; Doye & Hurt, 1997). In order to find new factors potentially involved in mRNA 3′-end formation, we have screened for mutations that confer synthetic lethality with a poly(A) polymerase temperature-sensitive mutant, *pap1-7*. We have restricted our analysis to mutations that conferred a temperature-sensitive phenotype because such mutants would likely display a deficient 3′-end processing activity on their own. We have isolated five synthetic lethal, temperature-sensitive *lcp* mutations (for lethal with conditional *pap1* allele). Here we report the cloning and characterization of *LCP5*. Surprisingly, this mutation impaired the processing of ribosomal RNA precursors, but showed normal pre-mRNA 3′-end processing activity.

Reprint requests to: Lionel Minvielle-Sebastia, Department of Cell Biology, Biozentrum, University of Basel, Klingelbergstrasse 70, CH-4056, Basel, Switzerland; e-mail: minvielle@ubaclu.unibas.ch.

The maturation of rRNA involves a complex series of modifications, notably pseudouridinylation, methylation, and both exo- and endonucleolytic cleavage events that lead to the formation of 18S, 5.8S, and 25S rRNAs. 18S maturation involves cleavage at three sites in the primary transcript, denoted A_0 to A_2. The pre-rRNA is processed at sites A_1 and A_2, 5′ and 3′ of the mature 18S rRNA, respectively. Cleavage at site A_2 separates the pathways for maturation of small and large ribosomal subunit rRNAs.

In *lcp5-1* cells the early cleavage steps A_0 to A_2 were affected. The mutant also showed reduced amounts of polysomes and a strong increase in free 60S ribosomal subunits due to decreased 40S levels. In addition, depletion of the protein in vivo inhibited pre-rRNA processing that led to a depletion of 40S subunits, a concomitant 60S accumulation, and decreased amounts of polysomes. Consistent with its role in pre-rRNA processing, we found that the Lcp5p protein is located in the nucleolus and is associated with snR17, the yeast homologue of snoRNA U3.

RESULTS

Synthetic lethal screen identifies a gene with unknown function

To identify further components of the pre-mRNA 3′-end processing machinery, a screen for synthetic lethal mutations with the poly(A) polymerase temperature-sensitive allele *pap1-7* was carried out (Fig. 1A). Mutant strains that did not grow in the absence of the wild-type *PAP1* gene were identified on plates containing 5-fluoroorotic acid [5-FOA; Figs. 1B,C]. We obtained 26 temperature-sensitive mutants. For five of them, tetrad analysis demonstrated a genetic linkage between the temperature- and 5-FOA-sensitive phenotypes. These mutations, termed *lcp1* to *lcp5*, are not linked to the plasmid-borne *pap1-7* allele and define five complementation groups (results not shown).

lcp mutations were isolated by several outcrosses with the W303 wild-type strain (see Table 1). Extracts were prepared from each of the mutant strains and tested for pre-mRNA 3′-end processing in vitro according to standard procedures (Minvielle-Sebastia et al., 1994). We found that extracts from all five mutants processed a ^{32}P-labeled pre-mRNA substrate to an extent comparable to a wild-type extract, even at elevated temperature (Fig. 2A; data not shown). These results suggested that the mutated genes were not coding for subunits of essential factors involved in mRNA 3′-end formation.

Below, we describe the characterization of *LCP5*. Wild-type *LCP5* was cloned by complementation of the temperature-sensitive phenotype of its corresponding mutant. Open reading frame YER127w (Mewes et al., 1997) was sufficient to render the cells temperature-resistant. The gene has been previously characterized by systematic Ty insertional analysis on chromosome V. Ty insertion in YER127w resulted in severe growth defects on rich medium (Smith et al., 1996). The protein has also been found to interact with Ngg1p in a two-hybrid screen (Martens et al., 1996). Ngg1p acts as a transcriptional coactivator/repressor and is involved in acetylation of nucleosomal histones. However, to the best of our knowledge no function has been assigned to YER127w so far.

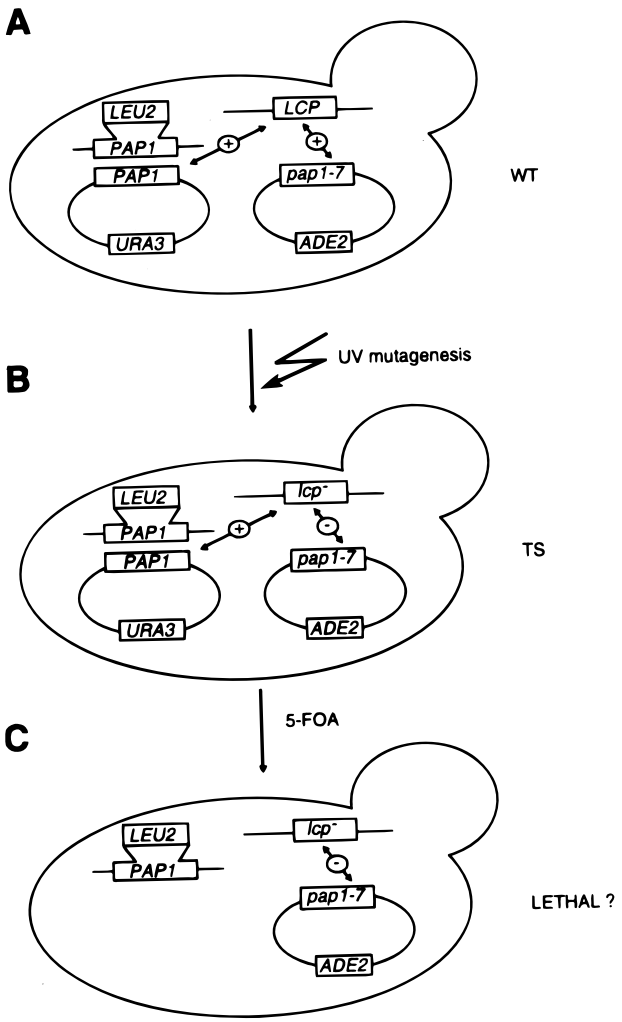

FIGURE 1. Schematic representation of the synthetic lethal screen with *pap1-7*. **A:** The starting strain, containing the *PAP1* disruption, the wild-type *PAP1* allele and the *pap1-7* allele. **B:** Genotype after UV mutagenesis in the presence of the wild-type *PAP1* gene. **C:** Resulting genotype after counterselection for the wild-type *PAP1* gene on 5-FOA plates. +: interaction supporting cell viability. −: aberrant interaction that fails to support cell viability. *LCP*: wild-type allele before UV mutagenesis, *lcp*$^-$: mutated allele after UV mutagenesis. *LEU2*, *ADE2*, *URA3*: selectable marker genes.

LCP5 is a single copy gene. It codes for a protein of 357 amino acids and has a calculated molecular mass of 40.8 kD. The predicted polypeptide has a high content of charged residues (33% D + E + K + R). Computational analysis detected a putative nuclear lo-

TABLE 1. Strains used in this study.

Strain	Relevant Genotype	Source
BMA41	Mat**a**/α, *ade2-1/ade2-1*, *leu2-3,112/leu2-3,112*, *ura3-1/ura3-1*, *trp1*Δ*/trp1*Δ, *his3-11,15/his3-11,15*, *can1-100/can1-100*	A. Baudin-Baillieu (Baudin-Baillieu et al., 1997)
JL17-3C	Mat**a**, *ade2-1*, *leu2-3,112*, *ura3-1*, *trp1-1*, *his3-11,15*, *can1-100*, *pap1::LEU2*, pHCp50 (*CEN4 URA3 PAP1*)	J. Lingner (Lingner, 1992)
JL17-3A	as JL17-3C, but Matα	J. Lingner (Lingner, 1992)
W303	*ade2-1*, *leu2-3,112*, *ura3-1*, *trp1-1*, *his3-11,15*, *can1-100*	R. Rothstein (Columbia University, New York)
YTW1	*ade2-1*, *leu2-3,112*, *ura3-1*, *trp1-1*, *his3-11,15*, *can1-100, lcp1-1*	this work
YTW4	*ade2-1*, *leu2-3,112*, *ura3-1*, *trp1-1*, *his3-11,15*, *can1-100, lcp4-1*	this work
YTW5	*ade2-1*, *leu2-3,112*, *ura3-1*, *trp1-1*, *his3-11,15*, *can1-100, lcp5-1*	this work
YTW6	Mat**a**/α *ade2-1/ade2-1*, *leu2-3,112/leu2-3,112*, *ura3-1/ura3-1*, *trp1*Δ*/trp1*Δ, *his3-11,15/his3-11,15*, *can1-100/can1-100, LCP5/lcp5*::*TRP1*	this work
YTW7	Mat**a**, *ade2-1*, *leu2-3,112*, *ura3-1*, *trp1*Δ, *his3-11,15*, *can1-100, lcp5::TRP1*, pFLH-lcp5-1 (*CEN4 HIS3 lcp5-1*)	this work
YTW10	Mat**a**, ade2-1, *leu2-3,112*, *ura3-1*, *trp1*Δ, *his3-11,15*, *can1-100, lcp5::TRP1,* pFLU-LCP5 (*CEN4 URA3 LCP5*)	this work
YTW11	*ade2-1*, *leu2-3,112*, *ura3-1*, *trp1*Δ, *his3-11,15*, *can1-100, lcp5::TRP1,* pGUR1-LCP5 (*CEN4 ADE2 Ubi-R-LCP5*)	this work
YTW12	Mat**a**/α *ade2-1/ade2-1*, *leu2-3,112/leu2-3,112*, *ura3-1/ura3-1*, *trp1*Δ*/trp1*Δ, *his3-11,15/his3-11,15*, *can1-100/can1-100, lcp5::TRP1/lcp5::TRP1*, pHH2-LCP5 (*CEN4 ADE2 HA-His*$_{12}$*-LCP5*)	this work
YDK2-7A	Matα, *ade2-1*, *leu2-3,112*, *ura3-1*, *trp1-1*, *his3-11,15*, *fal1::HIS3MX6*, pRS416 (*FAL1*, *URA3*)	P. Linder (Kressler et al., 1997)
Nop1-ProtA	Matα, *ade2*, *leu2*, *lys1*, *ura3*, *nop1::URA3* pUN100-ProtA-Nop1p	D. Tollervey (Jansen et al., 1993)
Gar1-ProtA	Mat**a**, *ade2*, *his3*, *lys2*, *trp1*, *ura3*, *URA3::GAL10::gar1* pMCGZZ1-ProtA-Gar1p	M. Caizergues-Ferrer (Ganot et al., 1997)

calization signal (Dingwall & Laskey, 1991) and a potential coiled coil region (Fig. 2B). The amino acid sequence of the protein shows similarities to a putative orthologue (accession No. SWISS-PROT: Q09713) in *Schizosaccharomyces pombe* (26.3% identity), and to a CCAAT enhancer-binding-like protein of *Caenorhabditis elegans* (Wilson et al., 1994).

LCP5 is essential for cell viability

To determine whether *LCP5* is an essential gene, a linear fragment in which 90% of the open reading frame (ORF) was replaced by the *TRP1* marker was transformed into the diploid BMA41 (see Materials and Methods). Integration at the correct locus was verified by Southern blot analysis for three transformants. Tetrad dissection revealed that only two of the four spores formed colonies on rich medium (results not shown). None of the viable spores could grow on minimal medium (SC) lacking tryptophan. To demonstrate that the gene is essential for vegetative growth, the *URA3*-marked centromeric plasmid pFLU-LCP5 (see Materials and Methods) bearing the wild-type *LCP5* gene was transformed into the diploid YTW6 carrying a heterozygous disruption of *LCP5*. Meiosis led to four viable spores on rich medium. Two of the four spores could grow on SC lacking tryptophan, but not on SC supplemented with 5-FOA. Taken together these results demonstrate that *LCP5* is essential for cell viability.

The *lcp5-1* mutation leads to 18S rRNA underaccumulation

Because extracts from *lcp5-1* cells showed wild-type mRNA 3′-end formation activity in vitro, we wanted to test whether mutant cells would show decreased steady state mRNA levels after a temperature shift (Minvielle-Sebastia et al., 1991). Total RNAs were isolated from *lcp5-1* mutant cells and from an isogenic wild-type sister spore. Remarkably, RNAs prepared from the

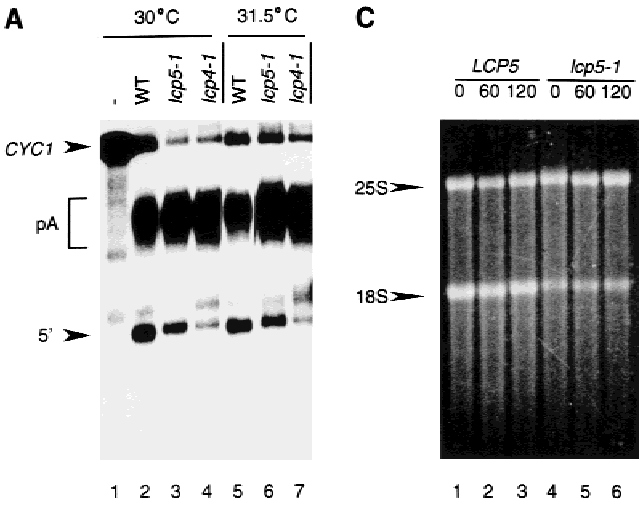

B

								10											20	
1	M	S	E	L	N	A	L	L	K	D	I	N	G	S	L	T	A	T	S	E
21	S	L	E	R	L	S	G	I	Y	S	N	S	A	T	D	E	I	P	E	S
41	N	Q	L	H	E	H	L	F	Y	D	A	K	K	P	A	E	K	V	S	L
61	L	S	L	K	N	G	S	M	L	G	Y	I	N	S	L	L	M	L	I	G
81	N	R	L	D	D	E	C	K	D	P	S	A	M	D	A	R	E	R	S	I
101	Q	H	R	V	V	L	E	R	G	V	K	P	L	E	K	K	L	A	Y	Q
121	L	D	K	L	T	R	A	Y	V	K	M	E	K	E	Y	K	D	A	E	K
141	R	A	L	E	K	S	T	L	V	N	H	S	G	N	D	D	S	E	D	D
161	E	S	S	E	D	E	I	A	Y	R	P	N	T	S	G	I	I	N	T	N
181	K	K	S	S	A	Y	R	V	E	E	T	A	K	Q	E	N	G	E	E	N
201	D	D	N	E	T	G	V	Y	K	P	P	K	I	T	A	V	L	P	P	Q
221	Q	T	H	F	E	D	R	F	D	A	R	E	H	K	D	R	S	N	K	S
241	R	M	Q	A	M	E	E	Y	I	R	E	S	S	D	Q	P	D	W	S	A
261	S	I	G	A	D	I	V	N	H	G	R	G	G	I	K	S	L	R	D	T
281	E	K	E	R	R	V	T	S	F	E	E	D	N	F	T	R	L	N	I	T
301	N	K	A	E	K	R	K	Q	K	Q	R	E	R	N	A	R	M	N	V	I
321	G	G	E	D	F	G	I	F	S	S	K	R	K	L	E	D	S	T	S	R
341	R	G	A	K	K	T	R	S	A	W	D	R	A	Q	R	R	L			
								10											20	

FIGURE 2. *lcp5-1* mutant is not affected in pre-mRNA 3′-end processing but shows underaccumulation of 18S rRNA. **A:** Cleavage and polyadenylation of the *CYC1* precursor RNA in vitro. The 3′-end processing activity of the wild-type (WT; lanes 2, 5), and the mutant extracts *lcp5-1* (lanes 3, 6) and *lcp4-1* (lanes 4, 7) were assayed under standard conditions (see Materials and Methods). The reactions proceeded for 70 min at 30 °C (lanes 1–4) and 31.5 °C (lanes 5–7). The positions of the *CYC1* precursor, the 5′ cleavage fragment, and polyadenylated species are indicated. **B:** Primary structure of Lcp5p. The predicted coiled coil region is boxed. Predicted, bipartite nuclear localization signals (NLSs) are underlined **C:** Electrophoretic separation of total RNA, isolated from wild-type (*LCP5*, lanes 1 to 3) and mutant *lcp5-1* cells (lanes 4 to 6). The cells were grown at room temperature and shifted to 37 °C for 0, 60, and 120 min (time indicated at the top). The position of mature 18S and 25S rRNA species is indicated.

temperature-sensitive strain grown at room temperature (RT) showed a substantial reduction of 18S rRNA compared to the wild-type control (Fig. 2C, compare lanes 1 and 4). After a temperature shift to 37 °C for up to 2 h, the 18S rRNA content did not decrease further (Fig. 2C, compare lanes 5 and 6 to lane 4). The decrease of 18S rRNA was likely responsible for the enhanced generation time of the *lcp5-1* mutant cells (Table 2). This observation suggested that *LCP5* could be involved in rRNA metabolism.

LCP5 is required for pre-rRNA processing

To verify that the mutant allele of the cloned gene was responsible for the observed phenotype, the gene was isolated by gap repair and its sequence was determined. The mutant Lcp5-1p exhibited a G197E mutation and a stop codon at position 209. The mutant allele was introduced in a strain bearing an *lcp5* null allele, rescued by pFLU-LCP5 (YTW10). The wild-type allele was counterselected on medium containing 5-FOA. The resulting strain, YTW7, was temperature sensitive and exhibited a decrease in the steady state 18S rRNA level comparable to the mutant isolated from the screen (results not shown). This experiment also confirmed that we actually isolated the wild-type allele *LCP5* from the genomic library by complementation of the *lcp5-1* mutant, and not a suppressor. In addition, a ubiquitin-Lcp5p fusion protein was cloned downstream of a repressible $P_{GAL10/CYC1}$ hybrid promoter (Jenny et al., 1996). In this construct, a ubiquitin moiety precedes an arginine, a haemagglutinin tag, a histidine tag and the ORF of *LCP5*. In vivo, the ubiquitin is cleaved off, exposing the arginine at the N-terminus of the polypeptide (hence called R-Lcp5p). According to the N-end rule, this confers instability to the polypeptide (Varshavsky, 1996). The construct was transformed into YTW10 cells, containing the *lcp5::TRP1* deletion rescued by pFLU-LCP5. After *URA3* counterselection on 5-FOA plates, the strain expressing R-Lcp5p (YTW11) grew on plates containing rich medium with 2% galactose, but not on plates containing 5% glucose (data not shown). In liquid cultures, a shift to glucose dramatically slowed down the cell growth after 10–12 h of incubation. RNAs extracted from glucose-shifted cells showed that in vivo depletion of Lcp5p decreased the 18S rRNA level to an extent similar to that of *lcp5-1* mutant cells (results not shown).

Several cleavage steps are required to generate mature 18S rRNA (see Fig. 3A). The primary transcript (35S) is cleaved at the site A_0 in vitro by the homologue of bacterial RNase III, Rnt1p (Elela et al., 1996). The pre-rRNA is processed at the 5′ end of the mature 18S rRNA and at the 3′ end in the internal transcribed spacer 1 (ITS1). Cleavage at site A_3 can be carried out in vitro by MRP RNase (Lygerou et al., 1996). Recent evidence suggests that processing steps A_0 to A_3 occur in a common complex in vivo (Allmang et al., 1996). It has previously been shown that inhibition of cleavage at sites A_0 to A_2 results in the accumulation of a 23S species (reviewed in Venema & Tollervey, 1995). Sim-

TABLE 2. In vivo phenotypes of strains.

Strain	Generation time[a] (YPAD) in min	Generation time[a] (SC) in min	%40S subunits of wild-type strain (RT)	%40S subunits of wild-type strain (37 °C)
YTW10 LCP5	156	219	100[b]	100[b]
YTW7 lcp5-1	381	700	23	17
YTW11 R-Lcp5p (GAL)	n.d.	360	82	n.d.
YTW11[c] R-Lcp5p (GLC)	—	—	10	n.d.

Generation times and 40S small ribosomal subunit content of strains used in this study. For analysis of ribosomal subunits at 37 °C, *lcp5-1* cells were grown at RT, harvested, and cultured overnight at the nonpermissive temperature.

[a]Doubling times were determined at 23 °C.

[b]The amount of 40S subunits in the wild-type strain was set to 100%.

[c]R-Lcp5p expressing cells were cultured overnight in YPAD, containing 5% glucose. Ratios were determined by calculating areas of subunit peaks after "run off" ribosomal subunit analysis as described in Materials and Methods.

n.d.: not determined.

ilarly, deletion of snR10 leads to the production of a 21S species (Tollervey, 1987; Morrissey & Tollervey, 1993). To determine why the 18S rRNA production was affected in *lcp5* mutants, RNAs were isolated from strains bearing a null allele of *lcp5* rescued either by the wild-type allele *LCP5*, or the temperature-sensitive allele *lcp5-1* isolated by gap repair, and also from the YTW11 strain expressing R-Lcp5p cultured for 8 h in glucose. We analyzed pre-rRNA processing intermediates by Northern blotting. An oligonucleotide complementary to a sequence upstream of the cleavage site A_0 (oligo 5′A_0) was used as a probe (Fig. 3B, panel A). In both the depleted (designated Glc) and the temperature-sensitive strains (*lcp5-1*) an aberrant RNA species comparable in size to the aforementioned 23S molecule was observed. Concomitantly, the 35S pre-rRNA precursor accumulated. The stronger accumulation of the 23S and 35S species in the depleted R-Lcp5p expressing strain was due to a more severe phenotype of this strain compared to the temperature-sensitive mutant. We then probed the same membrane with an oligonucleotide complementary to sequences between cleavage sites D and A_2 (oligo D/A_2). The 20S pre-rRNA processing intermediate was strongly reduced in the temperature-sensitive mutant, as well as in the strain depleted for Lcp5p (Fig. 3B, panel B). In addition, another aberrant RNA comparable in size to the 21S species was detected. When the same blot was hybridized with an oligonucleotide complementary to sequences between the cleavage sites A_2 and A_3 (oligo A_2/A_3), we found that the 27SA_2 intermediate was severely reduced upon depletion of Lcp5p or in the temperature-sensitive mutant *lcp5-1* (Fig. 3B, panel C). Finally, an oligonucleotide complementary to sequences between cleavage sites E and C_2 (oligo E/C_2) detected comparable amounts of 27S pre-rRNAs in the mutant, the wild-type, and the depleted strains, indicating that processing at site A_3 is not influenced by Lcp5p (Fig. 3B, panel D).

To determine whether the decrease in the steady state amount of 18S rRNA was a primary consequence of *LCP5* inactivation, RNAs were isolated after a short glucose shift of R-Lcp5p expressing cells and subjected to Northern blot analysis with probe A_2/A_3 (Fig. 4A). After only 35 min, 21S and 23S species accumulated in the RNAs of the culture grown in glucose (Fig. 4A, compare lanes 1 and 3). A decrease of the 27SA_2 intermediate was observed as well. Figure 4B shows that the reduction of Lcp5p protein concentration correlated with the pre-rRNA processing defects, as assessed by Western blot analysis. These results showed that depletion of Lcp5p or mutations in *LCP5* lead to predominant processing at site A_3, skipping the early cleavage steps at A_0 and A_2. The fast effects on pre-rRNA processing after glucose shift suggested that Lcp5p is directly involved in pre-rRNA maturation.

Efficient A_0 and A_2 cleavages are dependent on Lcp5p

Cleavage at individual sites was analyzed by primer extension. RNAs were isolated from strains expressing R-Lcp5p following growth in YP-Galactose (Gal) or YP-Glucose (Glc). Figure 5A shows the primer extension carried out with oligo E/C_2. Equal amounts of extension products up to cleavage sites B_{1L}, B_{1S} and A_3 were obtained (compare Fig. 5A, lanes 1–3 with lanes 4–6). In contrast, RNAs terminating at A_2 were strongly reduced after depletion of Lcp5p. Longer extension products were visible in all lanes demonstrating that the reduction was not due to artifactual

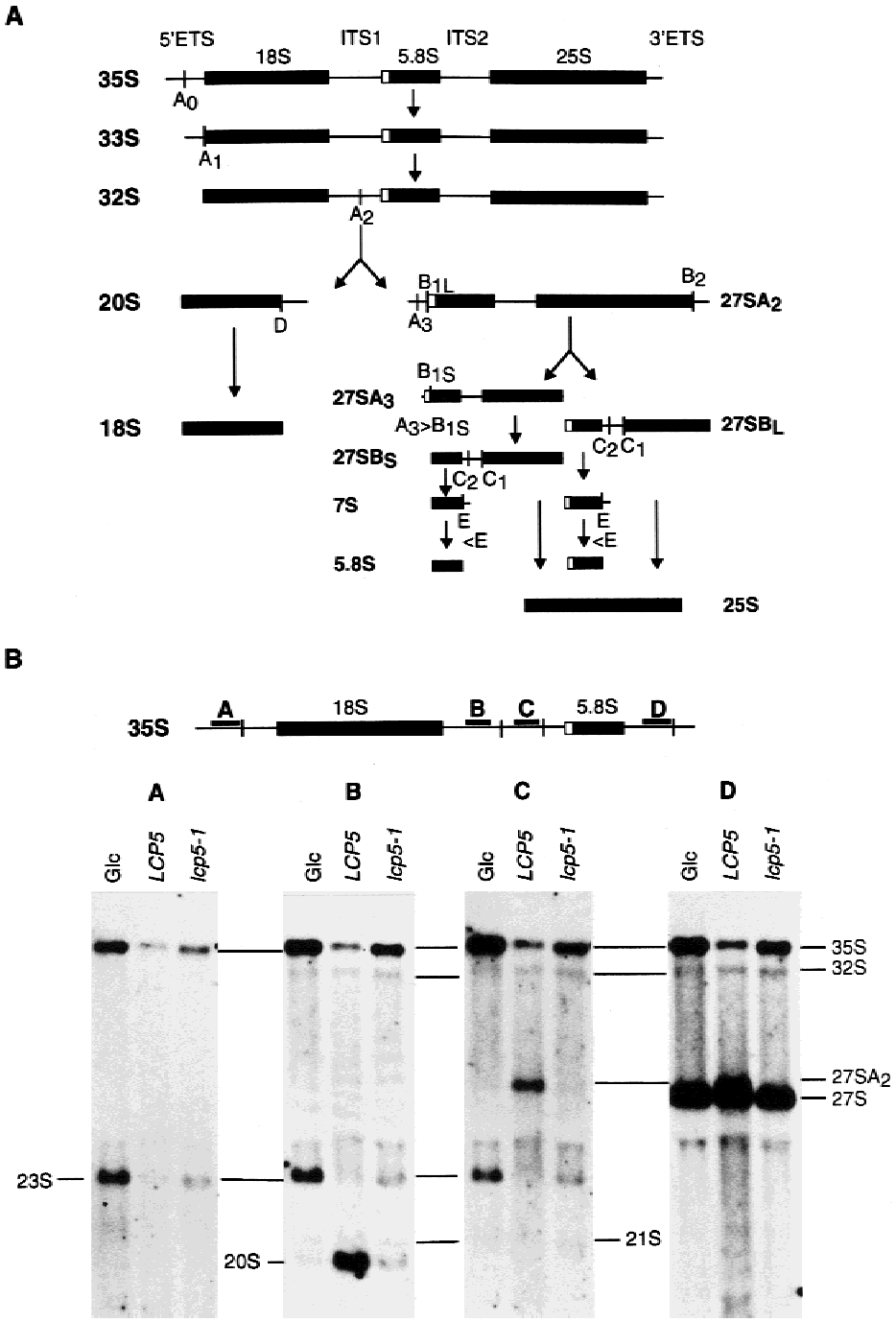

FIGURE 3. Aberrant pre-rRNA processing in *lcp5* mutants. **A:** Simplified overview of 35S pre-rRNA processing in yeast. Processing intermediates are designated with their respective sedimentation coefficient. Processing sites are indicated. >: exonucleolytic digestion up to the indicated site (adapted from Venema & Tollervey (1995)). **B:** Northern blots of RNA extracted from R-Lcp5p expressing cells shifted to 5% glucose for 8 h (Glc), wild-type cells grown in 5% glucose at 24 °C (*LCP5*) and *lcp5-1* mutant cells grown in 5% glucose at RT (*lcp5-1*). The labeled oligonucleotide used to probe the blot were: Panel A: oligonucleotide 5′ A_0; Panel B: oligonucleotide D/A_2; Panel C: oligonucleotide A_2/A_3; Panel D: oligonucleotide E/C_2. The positions of sequences recognized by the probes are indicated on the top. Processing intermediates and products are indicated.

inhibition of the reverse transcriptase. An oligonucleotide hybridizing immediately upstream of the A_1 cleavage site (Elela et al., 1996) was used in the primer extension shown in Figure 5B. We observed a reduced amount of A_0-cleaved RNAs, as well as accumulation of products extending to the transcription start site (compare Fig. 5B, lanes 1–3 with lanes 4–6). These results and those obtained from the Northern blot analyses demonstrated that the cleavage efficiency at sites A_0 and A_2 is reduced when Lcp5p is

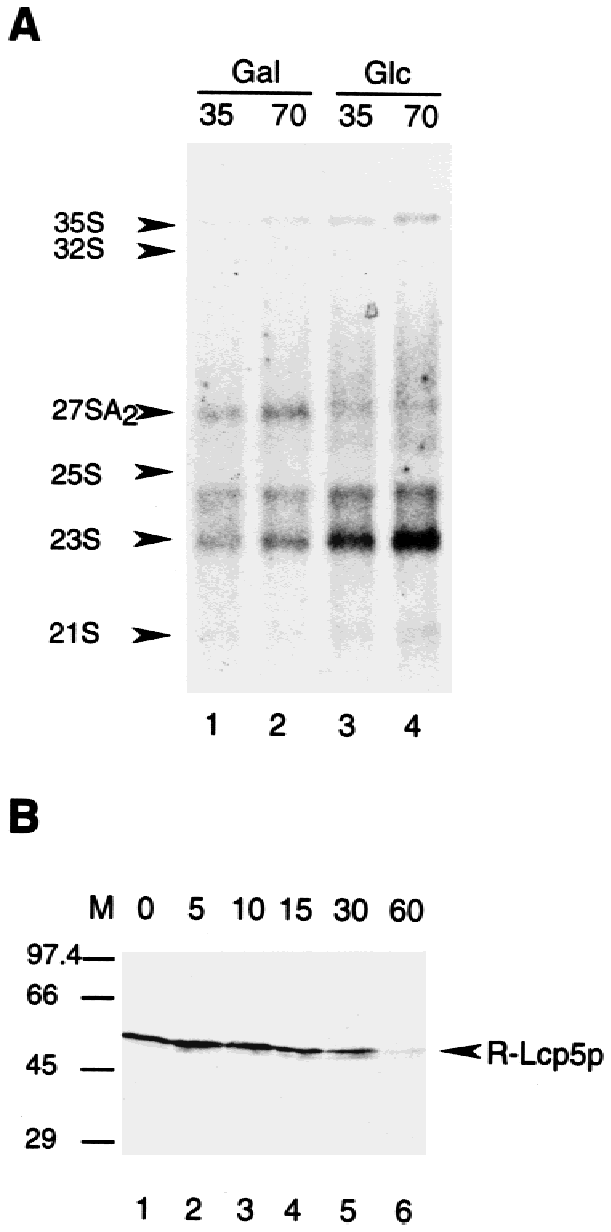

FIGURE 4. Pre-rRNA processing defects following in vivo depletion of Lcp5p. **A:** YTW11 cells expressing R-Lcp5p were grown in rich medium containing galactose and were transferred to rich medium containing either galactose (Gal; lanes 1 and 2) or glucose (Glc; lanes 3 and 4) for 35 and 70 min. Northern blot hybridization was performed with probe A_2/A_3. Arrowheads indicate processing intermediates and products. **B:** YTW11 cells expressing R-Lcp5p were grown on galactose and shifted to glucose. At the indicated times (in min after the glucose shift; top), total protein was extracted by heating in sample buffer, separated by SDS-PAGE, and Lcp5p was visualized by Western blot analysis. Affinity-purified anti-Lcp5p-antibody was used at a 1:5,000 dilution. Lane M: molecular weight markers in kDa.

inactivated, whereas processing at downstream sites remains largely unaffected.

Translation is affected in *lcp5* mutants

The reduction of 18S rRNA caused by *lcp5-1* mutations suggested an impairment in 40S ribosomal subunit biogenesis. The content of ribosomal subunits of mutant and wild-type cells was compared (see Materials and Methods). As predicted, the amount of 40S subunits relative to 60S subunits was reduced to 23% in *lcp5-1* cells (Table 2). To test whether this imbalance would lead to a defect in translation, *lcp5-1* mutant and wild-type strains were assayed for growth on rich medium containing the translation inhibitors paromomycin, neomycin and cycloheximide. Growth of mutant cells was inhibited at a neomycin concentration of 1 mg/ml, at a paromomycin concentration of 1 mg/ml, and at a cycloheximide concentration of 0.04 μg/ml, whereas the wild-type strain could still grow (T. Wiederkehr, unpubl. data). This suggested that translation is affected in the *lcp5-1* mutant strain.

The reduction of 40S subunit concentration suggested a defect in polysome formation. The polysome profiles of mutant and wild-type cells were determined in low-salt buffer (Fig. 6). In the mutant, polysome peaks were strongly reduced. Because of the depletion of 40S ribosomal subunits, a large peak of free 60S subunits overlapped with the monosome peak (compare Fig. 6A with 6B). To demonstrate that depletion of 40S ribosomal subunits was a direct consequence of mutations in *lcp5*, R-Lcp5p expressing cells were grown on YP-Galactose and transferred to YP-Glucose for three hours. The polysome profile of the Lcp5p-depleted cells showed a decrease in 40S ribosomal subunits, as a consequence an increase in free 60S ribosomal subunits and a decrease in polysomes (compare Fig. 6C with 6D). The strength of the observed phenotype was in good agreement with the levels of 18S rRNA as judged by ethidium–bromide staining of denaturing agarose gels (results not shown). These results support the conclusion that due to defective pre-rRNA processing, assembly of 40S ribosomal subunits and translation are affected by *lcp5-1* mutations.

Lcp5p is predominantly located in the nucleolus

The subcellular localization of Lcp5p was assessed by indirect immunofluorescence on wild-type cells. A strong signal was observed in the nucleus (Fig. 7A; see Fig. 7D for phase contrast), as well as a weak background of cytoplasmic staining. When the same cells were stained with DAPI (Fig. 7B), it became clear that the signal of Lcp5p antibodies was confined to part of the nucleus where DAPI staining was less intense (see Fig. 7C for an overlay of Figs. 7A and 7B), suggesting that the Lcp5p antibodies decorated the nucleolus. To confirm this observation, a diploid strain expressing HA-tagged Lcp5p was prepared for immunofluorescence, as described in Materials and Methods. As a control for nucleolar staining, monoclonal antibody (mAb) A66 directed against Nop1p, the yeast homologue of fibrillarin (Schimmang et al., 1989),

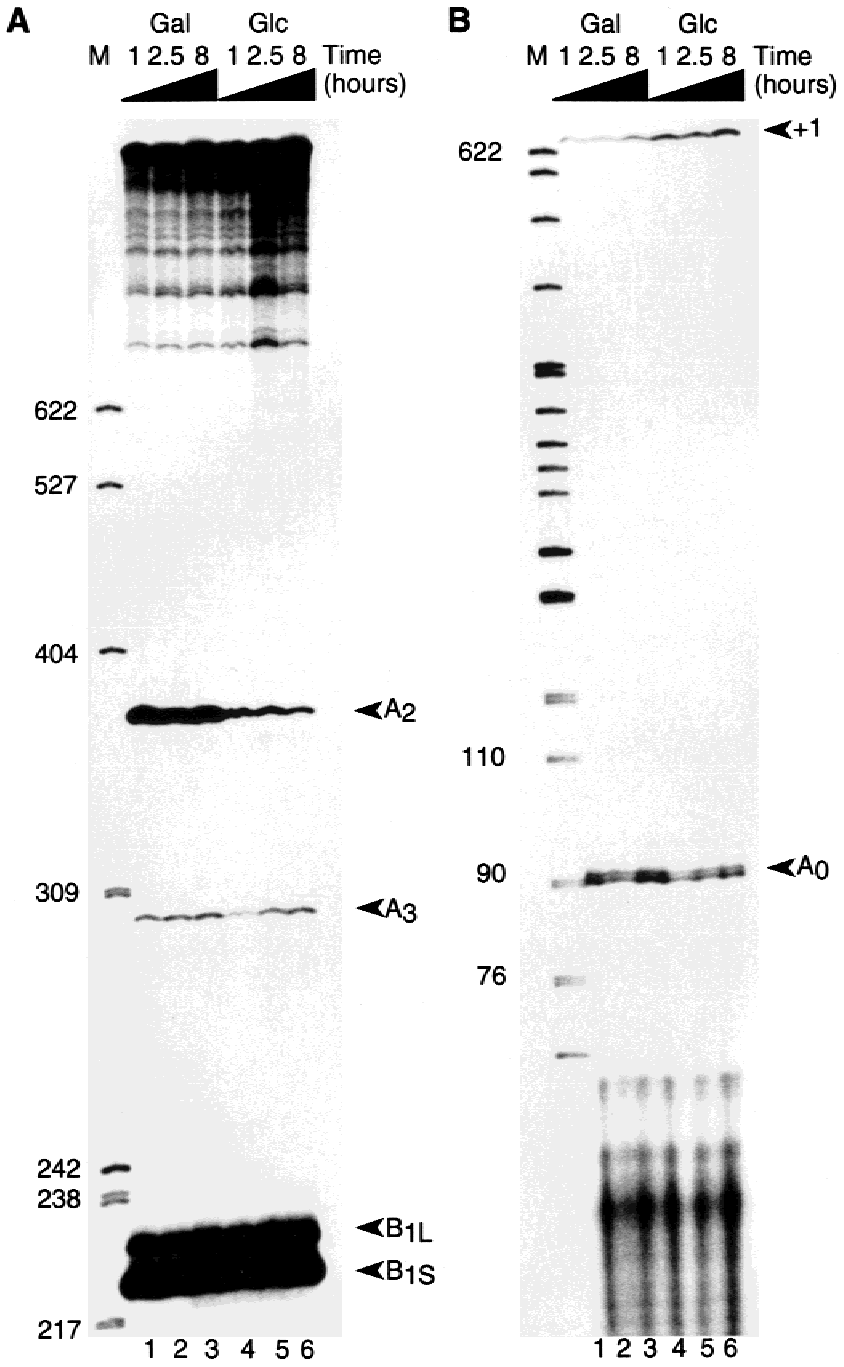

FIGURE 5. Lcp5p depletion affects pre-rRNA processing at sites A_0 and A_2. **A:** R-Lcp5p expressing cells were grown on YP-Galactose and transferred to either YP-Galactose (Gal, lanes 1 to 3) or YP-Glucose (Glc, lanes 4 to 6) for the indicated times (in hours, top). RNA was extracted and subjected to primer extension with oligonucleotide E/C_2. Extensions to sites B_{1L}, B_{1S}, A_2 and A_3 are indicated. **B:** As in A except that oligonucleotide $5'A_1$ was used to detect A_0-cleaved species. Extension up to the transcription start (+1) and extension up to site A_0 are indicated. The products were separated on denaturing 6% polyacrylamide/8.3 M urea gels. Labeled Hpa II-restricted pBR322 fragments were used as size markers (lane M, in nucleotides).

was used at the same time as affinity-purified antibodies directed against Lcp5p. Confocal microscopy showed that the signals of Nop1p and Lcp5p overlapped (Fig. 7E,F; see Fig. 7G for an overlay) and demonstrates that Lcp5p resides in the nucleolus. In addition, antibodies directed against the HA epitope were used in combination with antibodies against a bona fide nucleoplasmic protein, poly(A) polymerase (Pap1p). Whereas antibodies against Pap1p uniformly stained the nucleus, the antibodies directed against the HA epitope localized Lcp5p in a more restricted, crescent-shaped region of the nucleus (Fig. 7I; see Fig. 7J for an

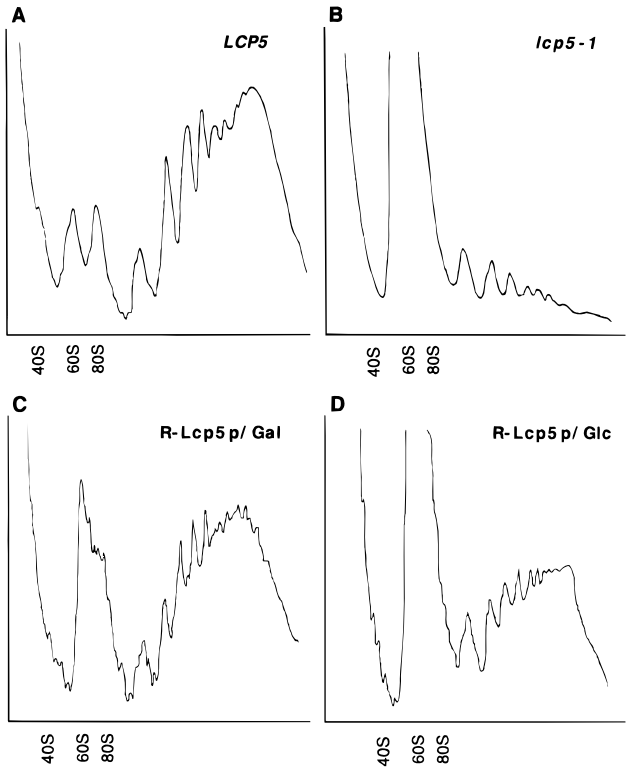

FIGURE 6. Aberrant polysome formation in *lcp5* mutants. Polysome profiles recorded from deletion strains rescued by *LCP5* (**A**) or *lcp5-1* (**B**) grown at permissive temperature. Polysome profiles from R-Lcp5p expressing cells grown on YP-Galactose and transferred either to YP-Galactose (**C**) or YP-Glucose (**D**) for three hours. The positions of 40S and 60S ribosomal subunit peaks, as well as the position of the 80S monosome peak are indicated.

overlay). The absence of nucleoplasmic and cytoplasmic staining with the antibodies directed against the HA epitope suggested that the signal obtained with affinity-purified polyclonal antibodies may be due to a cross-reactivity with an unrelated polypeptide. These results showed that Lcp5p is predominantly located in the nucleolus.

Lcp5p is associated with U3 snoRNA

In addition to protein factors, formation of 18S rRNA requires snoRNAs snR10, snR17 (U3), snR30 and snR128 (U14). To determine whether Lcp5p is associated with snoRNAs, we carried out immunoprecipitation with antibodies directed against Lcp5p and extracted potentially associated RNAs (see Materials and Methods). As positive controls, extracts from strains expressing protein A-tagged fusions of Gar1p and Nop1p were prepared. The precipitates from both control polypeptides contained snR10, U3, snR30 and U14 (Fig. 8, lanes 2,3). Interestingly, antibodies directed against Lcp5p precipitated exclusively U3, whereas none of the tested snoRNAs precipitated with the pre-immune serum (Fig. 8, compare lanes 4 and 6 with lanes 5 and 7). The interaction between Lcp5p and U3 is likely to be specific because significant amounts of U3 could be recovered even after extensive washes with 300 mM NaCl (Fig. 8, lane 6). In the same conditions, an unrelated protein A-tagged fusion (Nsp1p) did not precipitate any RNA (data not shown).

fal1 and *lcp5-1* mutant alleles are synthetic lethal

Recently, Kressler et al. (1997) have shown that *FAL1* is required for 18S rRNA processing. We crossed a deletion mutant of *fal1*, rescued by the wild-type allele on a centromeric plasmid (containing the *URA3* gene) with a strain harboring an *lcp5* deletion, rescued by the plasmid borne mutant *lcp5-1*. After meiosis, we isolated a strain that contained both chromosomal disruptions rescued by the wild-type *FAL1* gene and the mutant allele *lcp5-1*. The cells were transformed with centromeric plasmids containing either *fal1-1* or *fal1-9* mutant alleles (Kressler et al., 1997; D. Kressler, J. de la Cruz, M. Rojo, & P. Linder, pers. comm.). Independent transformants were streaked on minimal medium supplemented with 5-FOA or on medium lacking the drug (Fig. 9). None of the double mutants *fal1-1 lcp5-1* nor *fal1-9 lcp5-1* could grow in the presence of the drug, whereas the growth rates of the mutant *fal1* strains by themselves were not significantly reduced (results not shown). This synthetic lethality provides additional evidence that Lcp5p participates in the processing of pre-rRNAs.

Cumulatively, the experiments described above strongly support the conclusion that Lcp5p is a new essential component of the nucleolar pre-rRNA processing machinery.

DISCUSSION

We have identified a new protein (Lcp5p) involved in pre-rRNA processing. The *LCP5* gene has been found in a screen for synthetic lethal mutations with the temperature-sensitive allele of poly(A) polymerase, *pap1-7*. Several experiments showed that Lcp5p is not essential for pre-mRNA 3′-end processing. First, extracts prepared from the *lcp5-1* mutant were active in vitro for cleavage and polyadenylation. Second, immunodepletion of wild-type extracts with antibodies directed against Lcp5p did not lead to inactivation of the 3′-end processing activity (results not shown). In addition, a temperature shift of *lcp5-1* cells to 37 °C for 2 h did not cause a strong reduction of the steady state level of *ACT1* mRNA (results not shown). In contrast, temperature-sensitive mutations in genes coding for the 3′-end processing components Rna14p, Rna15p and Fip1p (Minvielle-Sebastia et al., 1991; Minvielle-Sebastia et al., 1994; Preker et al., 1995) did not allow accumulation of the *ACT1* mRNA after shifting the mutant cells to the nonpermissive temperature. Finally,

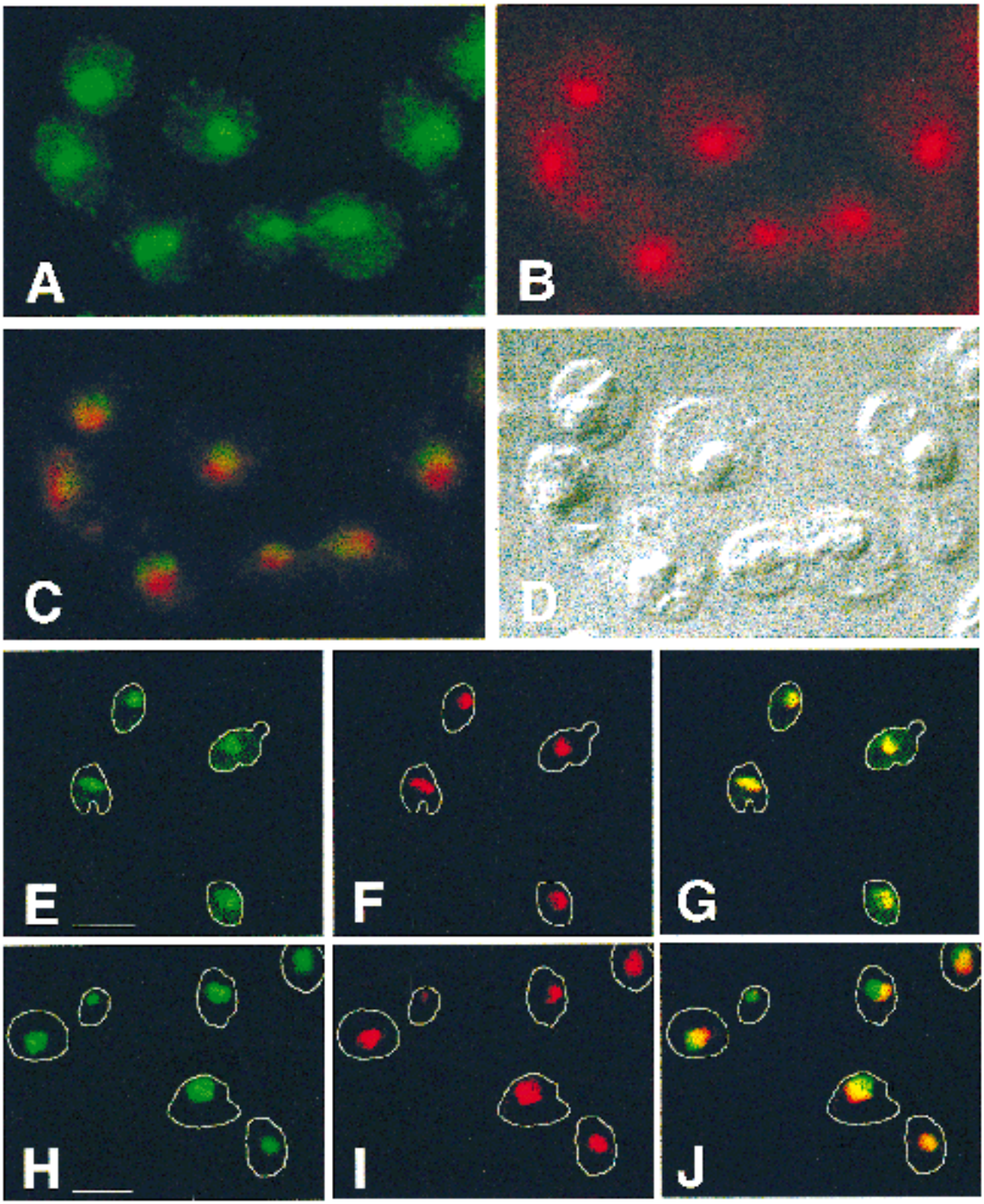

FIGURE 7. Nucleolar localization of Lcp5p by indirect immunofluorescence. Lcp5p was localized in the wild-type strain BMA41 (**A**–**D**) and with confocal microscopy in the strain YTW12 expressing an HA-histidine-tagged fusion of Lcp5p (**E**–**J**). **A**: Cells were decorated with affinity-purified antibodies directed against Lcp5p. **B**: DAPI staining (see Materials and Methods). **C**: Overlay of DAPI staining (red) and Lcp5p staining (green). Red color was assigned to the DAPI signal. **D**: Nomarski phase contrast. **E**,**H**: Affinity-purified antibodies directed against Lcp5p and Pap1p, respectively. **F**,**I**: Monoclonal antibodies directed against Nop1p and the HA epitope, respectively. **G**: Overlay of Nop1p (red) and Lcp5p (green) staining. **J**: overlay of Pap1p (green) and Lcp5p (red) staining. The outline of the cells and a scale bar (5 μm, **E** and **H**) are depicted for the confocal panels.

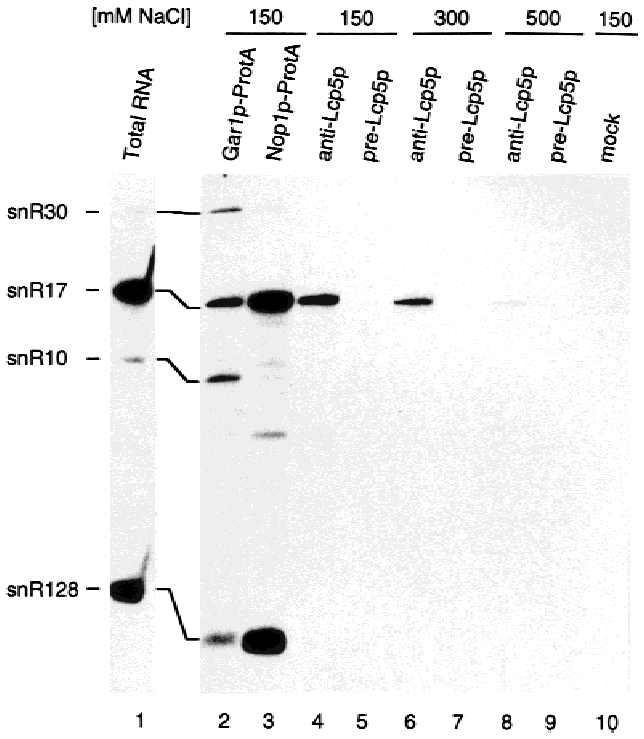

FIGURE 8. Antibodies directed against Lcp5p precipitate U3 snoRNA. Immunoprecipitation was performed with protein A-tagged fusions of Gar1p (lane 2), Nop1p (lane 3), and with antibodies directed against Lcp5p (lanes 4, 6 and 8) or its cognate preserum (lanes 5, 7 and 9) at the indicated salt concentration (top). Lane 10: Mock precipitation without antibody. Precipitated RNAs were subjected to Northern hybridization with oligonucleotides complementary to snR10, snR17, snR30 and snR128.

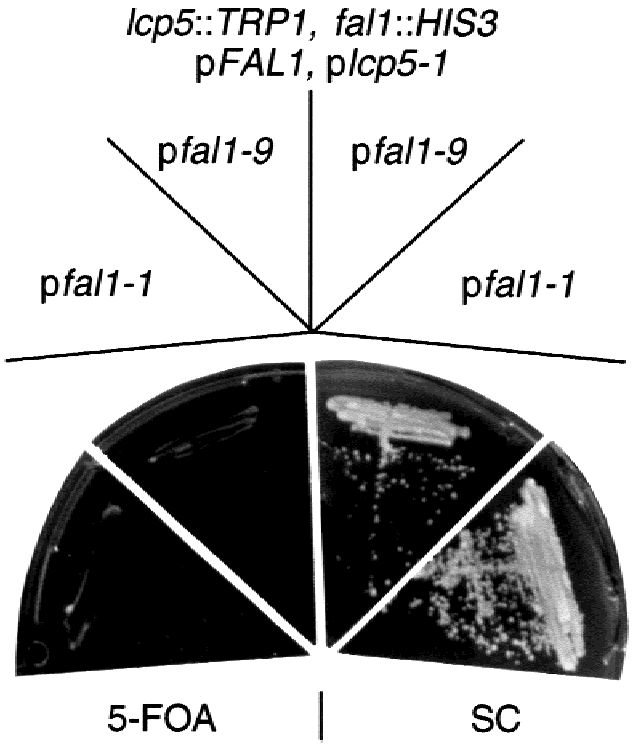

FIGURE 9. Synthetic lethality of *fal1* and *lcp5* mutant alleles. Strains deleted for both *fal1* and *lcp5* rescued by the wild-type *FAL1* gene and the mutant alleles *lcp5-1*, *fal1-1* or *fal1-9* (on centromeric plasmids) were streaked on SC or 5-FOA-containing SC-plates. Plates were incubated at 24 °C.

Lcp5p has not been found among the polypeptides that copurify with the essential 3′-end processing factors (Kessler et al., 1996; Kessler et al., 1997; Minvielle-Sebastia et al., 1997; Preker et al., 1997; Zhao et al., 1997).

Instead, our results showed that the *LCP5* gene product is required for ribosomal RNA maturation. This conclusion was supported by the observation that rRNA isolated from the strain expressing R-Lcp5p under the control of a repressible promoter accumulated aberrant processing species after a shift to glucose compared to a control grown in galactose. Upon glucose shift, pre-rRNA processing was rapidly affected leading to an inhibition of cleavage at processing sites A_0 to A_2, as indicated by the accumulation of 23S and 21S aberrant processing species. Similar effects have been observed by depletion of snoRNP components that are required for 18S rRNA maturation (Li et al., 1990; Hughes & Ares, 1991; Morrissey & Tollervey, 1993; Beltrame & Tollervey, 1995; Venema & Tollervey, 1996). An overnight glucose shift of R-Lcp5p-expressing cells resulted in a depletion of 18S rRNA comparable to the level observed with the temperature-sensitive *lcp5-1* strain (results not shown). Furthermore, the inhibition of pre-rRNA processing seems to be a direct effect of the depletion of the protein, because aberrant processing intermediates already accumulated above the control levels after about half an hour of glucose repression.

To test whether Lcp5p could be involved in methylation of the pre-rRNA and indirectly affect its processing, we performed a pulse-chase labeling with ^{3}H-methionine. R-Lcp5p expressing cells were shifted for three hours to YP-Glucose before the pulse-chase labeling. Northern-blot analyses showed accumulation of labeled 35S precursor and a lower abundance of 18S rRNA suggesting that the aberrant processing was not due to an overall methylation defect (results not shown).

The apparent similarity of Lcp5p to a CCAAT enhancer-binding-like protein and the identification of the ORF in a two-hybrid screen with Ngg1p would have suggested a role in transcriptional activation. To the best of our knowlegde, no further experimental data hint at an involvement of Lcp5p in this process. However, either the in vivo depletion of Lcp5p or its inactivation by a temperature-sensitive mutation led to the accumulation of unprocessed rRNA processing intermediates. In addition, we have shown that *FAL1* and *LCP5* interact genetically, suggesting a primary involvement of Lcp5p in pre-rRNA processing.

As expected from a defective 18S rRNA production, the mutant *lcp5-1* showed reduced amounts of 40S

ribosomal subunits and hypersensitivity to aminoglycosidic antibiotics (neomycin and paromomycin) and to cycloheximide. Hypersensitivity to paromomycin has been reported for mutants in *NSR1*, the putative yeast nucleolin homologue (Lee et al., 1992) and in *FAL1* (Kressler et al., 1997). As a result, both gene products were shown to be involved in 18S rRNA maturation. Aminoglycosidic antibiotics inhibit early steps in translation (Eustice & Wilhelm, 1984b), act as suppressors of nonsense codons (Palmer et al., 1979; Singh et al., 1979) and cause misreading in translation (Eustice & Wilhelm, 1984a). Cycloheximide binds to the 60S ribosomal subunit and inhibits both initiation and elongation of translation (Hampsey, 1997). The observed hypersensitivity is consistent with a defective translation initiation in *lcp5* mutants as a consequence of a reduced amount of 40S ribosomal subunits. Polysome profile analyses confirmed that translation is impaired in *lcp5-1* mutants. Almost all the ribosomal subunits were present in subpolysomal fractions. The low number of free 40S ribosomal subunits due to deficient 18S rRNA formation probably prevents efficient polysome formation (see Table 2). Therefore, antibiotics that lead to aberrant translation products or inhibit initiation of translation enhance the mutant phenotype beyond a tolerable level. It is likely that the enhanced turnover of R-Lcp5p in vivo, even when cells were cultured in YP-Galactose, led to an increase in free 60S ribosomal subunits and 80S monosomes compared to the wild-type control (compare Fig. 6A with 6C). This is in agreement with Northern-blot analyses of R-Lcp5p expressing cells (compare Fig. 4A, lanes 1 and 2, to Fig. 3B, panel C, lane *LCP5*). The amount of 18S rRNA correlates well with the strength of the observed phenotypes (results not shown).

Biochemical and genetic analyses have shown that poly(A)-bound Pab1p binds to the initiation factor eIF4G (Tarun & Sachs, 1996; Tarun et al., 1997) which in turn recognizes the 5′ cap structure via the cap binding protein eIF4E (Haghighat & Sonenberg, 1997). Recently, it has also been shown that mRNAs with shorter poly(A) tracts are shifted towards monosomes in polysome profiles of mutant *pap1-1* cells when ribosomal subunits are depleted at the same time (Proweller & Butler, 1997). Similarly, a more severe depletion of the 40S small ribosomal subunit because of pre-rRNA processing defects, as observed in *lcp5* mutants, could lead to inefficient translation and eventually to cell death in the *lcp5-1 pap1-7* double mutant. Other experiments also suggested that synthetic lethality between *pap1* and *lcp5-1* mutants is allele dependent. We found that the reduction in the poly(A)-tail length of some of our *pap1* mutant alleles correlated with hypersensitivity to translation inhibitors, mutant polysome profiles, and synthetic lethality with *lcp5-1* at any temperature (T. Wiederkehr, P.J. Preker, & L. Minvielle-Sebastia, in prep.). However, we cannot exclude that additional defects, like the mRNA stability of specific transcripts, contribute to the synthetic lethality.

We have demonstrated that Lcp5p is present in the nucleolus because Nop1p and Lcp5p antibodies decorated the same crescent-shaped regions previously shown to correspond to yeast nucleoli (Guthrie & Fink, 1991). Furthermore, detection of Pap1p in the nucleus was weaker in regions where the Lcp5p signal was located.

We have shown that snR17 is tightly associated with Lcp5p and that none of the other snoRNAs snR10, snR128, and snR30, were precipitated in the same experiment. Upon temperature shift of the mutant *lcp5-1* or after depletion of the protein in the R-Lcp5p expressing strain, no decrease in the steady-state levels of snR17 or snR128 was detected (results not shown). Sof1p was the first protein in *Saccharomyces cerevisiae* to be found associated with U3 snoRNA (Jansen et al., 1993). Recently, another component of U3 snoRNP in yeast, Mpp10p, has been identified (Dunbar et al., 1997). Like Lcp5p, immunoprecipitation of Mpp10p and Sof1p precipitates snR17.

Further experiments are underway to examine whether Lcp5p is directly associated with other components of the U3 snoRNP. Our results reported here demonstrate that Lcp5p is a novel essential protein required for rRNA maturation, and suggest that not all the factors involved in this complex processing reaction have been uncovered yet.

MATERIALS AND METHODS

Yeast strains, media, and genetic methods

The *S. cerevisiae* strains used in this study are listed in Table 1. Media and genetic methods were as described elsewhere (Guthrie & Fink, 1991). Yeast cells were transformed by treatment with lithium acetate and polyethylene glycol (Gietz et al., 1992).

Synthetic lethal screen

The strain JL17-3C was transformed with pApap1-7 (Minvielle-Sebastia et al., 1994). About 7×10^4 transformants were spread on 42 SC plates, lacking adenine, uracil and leucine. UV irradiation was carried out with a handheld germicidal light at 254 nm for 80 s at a distance of 50 cm. Viable colonies (1×10^4) were replica-plated on SC supplemented with 5-FOA. About 0.5% of the cells were not able to grow in the absence of pHCp50, containing *PAP1* (see Table 1). The mutants were restreaked and tested for the temperature-sensitive and 5-FOA-sensitive phenotypes. The temperature-sensitive mutation *lcp5-1* was isolated by four outcrosses to W303.

Cloning of *LCP5* and disruption

Strain YTW5, containing the temperature-sensitive allele *lcp5-1* was transformed with a genomic library constructed in the

centromeric plasmid pFL39 (a gift of François Lacroute). Several thousand transformants were replica-plated onto rich medium at 37 °C. One temperature-resistant colony was picked, restreaked, the plasmid was isolated, and the genomic insert sequenced at both ends. We used the tFASTA algorithm (Pearson & Lipman, 1988) to obtain the complete sequence information of the complementing genomic region (accession No. L11119; EMBL). The genomic region was analyzed for complementation by cloning restriction fragments into pFL39 and transformation into *lcp5-1* mutants. As a consequence a fragment containing YER127w as the only detectable ORF-coding gene was identified. For disruption, a genomic fragment containing *LCP5* was cloned into pUC19. A *TRP1* marker cassette was introduced between a N-terminal *Nsi* I and a C-terminal *Bbs* I site. The deletion construct was cut from pUC19 by restriction at two flanking sites in the polylinker and directly used to transform BMA41 cells.

Synthetic lethality of *fal1* alleles and *lcp5-1*

Strain YDK2-7A was crossed to strain YTW7, the diploids were sporulated and tetrads were dissected. A spore containing the chromosomal disruptions *fal1::HIS3MX6* and *lcp5::TRP1* was transformed with the mutant alleles *fal1-1* and *fal1-9* on centromeric plasmids (Kressler et al., 1997). Transformants were streaked on SC- or 5-FOA-containing SC-plates.

Plasmids

Plasmids were constructed by standard procedures (Sambrook et al., 1989). pFL39-LCP5 was derived from the complementing plasmid by *Pst* I/*Bam*H I digestion and religation. pFLU-LCP5 was derived from pFL39-LCP5 by exchanging the *TRP1* marker with a *URA3* marker. pGM-LCP5 was constructed by cutting pGM10 (Martin & Keller, 1996) with *Nde* I/*Bam*H I and inserting an *Nde* I/*Bam*H I genomic fragment containing the C-terminus of Lcp5p and 3′ untranslated sequences. The *Nde* I site was used to insert the N-terminus of Lcp5p by PCR with the primers 5′-LCP5: GGGAATTC CATATGTCTGAACTTAATGCATTATTA/ 3′-LCP5: CTACAG TCTCCTTTGAGCTCTATCCCAGGC and overnight digestion with *Nde* I. The resulting plasmid was cut with *Nsi* I/*Bam*H I and an *Nsi* I/*Afl* III fragment of pFL39-LCP5 covering most of the open reading frame was inserted. For the construction of pGUR1-LCP5, a PCR fragment containing flanking *Not* I sites (Primer 5′ rGAL-LCP5: AAGGAAAAAAGCGGCCGCGAG AGGGAGTCACCATCACCATCACCATAT/ 3′ rGAL-LCP5: T TCCTTTTTTGCGGCCGCCTACAGTCTCCTTTGAGC) was amplified from pGM-LCP5, and inserted into the *Not* I site of pGUR1 (Jenny et al., 1996). pHH2-LCP5 was constructed by inserting the *Not* I cassette of pGUR1-LCP5 containing a histidine tag and the ORF of Lcp5p into *Not* I restricted pHH2 (centromeric vector containing an HA- and a histidine tag; L. Minvielle-Sebastia, unpubl. vectors). The resulting construct contains an HA- and two consecutive histidine tags. For gap repair the complementing plasmid was cut with *Pst* I and religated. The resulting vector was linearized with *Bam*H I/*Apa* I digestion and transformed into *lcp5-1* mutant cells. Transformants were temperature sensitive and the plasmid was recovered by yeast plasmid DNA preparation and electrotransformation into *Escherichia coli* according to established procedures (Guthrie & Fink, 1991).

RNA isolation, blotting, and primer extension

RNAs were extracted from strains grown in YPAD to an OD_{600} of ~1. For temperature shift, an equal volume of prewarmed (51 °C) medium was added and the culture was incubated at 37 °C. Aliquots corresponding to 10 OD_{600} were removed. For the galactose-glucose shift, cells were grown in YP-Galactose to an OD_{600} of 0.07–0.5, the culture was centrifuged, resuspended in YP, split in two parts, and the sugar concentration was adjusted to either 5% glucose or 2% galactose. Aliquots corresponding to 3.5–10 OD_{600} were withdrawn at the times indicated and added to an equal volume of crushed ice. After centrifugation at 4 °C, the cells were washed with 1 ml of cold water and cell pellets were frozen on dry ice. RNA was isolated with hot acidic phenol (Collart & Oliviero, 1994). Equal amounts of total RNA (5 μg) were separated on 1.2% formaldehyde/agarose gels or used without further treatment for primer extensions. Northern blotting, hybridization, and primer extension were done according to published procedures (Venema & Tollervey, 1996; Kressler et al., 1997). The sequences of the primers are: Oligonucleotide 5′ A_0: GGT CTCTCTGCTGCCGG, oligonucleotide A_2/A_3: TGTTACCTC TGGGCCC, Oligonucleotide D/A_2: CGGTTTTAATTGTCCTA, Oligonucleotide E/C_2: GGCCAGCAATTTCAAGTTA, Oligonucleotide 5′A_1: ACTATCTTAAAACAAGCAACAAGCAG (Elela et al., 1996). For probing of snoRNAΔ the following oligonucleotides were used (Kressler et al., 1997): Oligonucleotide anti-snR10: CCTTGCAACGGTCCTCATCCGGG, oligonucleotide anti-snR17: TTCGGTTTCTCACTCTGGGGTAC, oligonucleotide anti-snR30: GAAGCGCCATCTAGATG, oligonucleotide anti-snR128: GGAACCAGTCTTTCATCACC.

Polysome analysis

Polysomes were prepared according to Kressler et al. (1997). To 200-ml cultures of yeast cells (OD_{600} = 0.4–1) in YPAD, 100 μg/ml cycloheximide was added, mixed, and the cells were kept on ice for 5 min. The cells were harvested, washed in lysis buffer (10 mM Tris-HCl [pH 7.5 (24 °C)], 100 mM NaCl, 30 mM $MgCl_2$, 100 μg/ml cycloheximide, and 200 μg/ml heparin), centrifuged, and resuspended in 1 ml lysis buffer. After a 10-s centrifugation, the cells were resuspended in 3 volumes of lysis buffer, 1 volume of glass beads was added, and the cells were broken by vortexing eight times for 30 s. Between vortexing, the cells were kept on ice for 30 s. The lysate was centrifuged for 10 min at 4 °C, 1/10 volume of 80% glycerol was added, and the extract was frozen in liquid nitrogen. 0.2–0.4 ml (OD_{260} = 25–40) were loaded onto 12 ml 15.7–54% (w/v) sucrose (Bio-Rad) gradients made up in 50 mM Tris-acetate [pH 7.5 (24 °C)], 50 mM NH_4Cl, 12 mM $MgCl_2$, 1 mM DTT, and 100 μg/ml heparin. The gradients were spun at 39,000 rpm (204,000 × *g*) for 165 min in a TST41.14 rotor at 4 °C. The gradients were unloaded and the OD_{254} was continuously monitored. For determination of ribosomal subunit and monosome peaks in the elution profile, fractions were collected and RNA was extracted and analyzed for 18S and 25S rRNA contents. For analysis of ribosomal subunits, cells were grown as above, sodium azide

was added to the culture to a final concentration of 1 mM, the cells were shaken for 15 min and harvested and extracted as above. Lysis buffer consisted of 50 mM Tris-HCl [pH 7.4 (24 °C)], 50 mM NaCl, and 1 mM DTT. The extracts were loaded onto 7–50% (w/v) sucrose gradients made up in lysis buffer. The gradients were centrifuged for 210 min at 39,000 rpm in a TST41.14 rotor at 4 °C. The gradients were unloaded and the OD_{280} was continuously monitored.

Expression of recombinant protein and production of antibodies

pGM-LCP5 was used to transform BL21(DE3)LysS cells (Studier, 1991). The histidine-tagged protein was purified on Ni^{2+}-nitrilotriacetic-acid-agarose (Qiagen) columns according to the manufacturers' instructions for denaturing purification of proteins. A rabbit was injected with 50–100 μg of gel-purified protein in a 1 ml volume containing 50% adjuvant (Specol). Affinity purification was done by adsorption of antiserum to nitrocellulose pieces (Schleicher & Schuell) blotted with recombinant Lcp5p protein, subsequent elution in acidic buffer and neutralization (Harlow & Lane, 1988).

Pre-mRNA 3′-end processing activity

Preparation of cell extracts and in vitro 3′-end processing assays were done as described (Minvielle-Sebastia et al., 1994).

Computational analysis

For the prediction of coiled coil regions and nuclear localization signals we used the programs COILS (Lupas et al., 1991) and PSORT (Nakai & Kanehisa, 1992), respectively. Both are available in the menu TOOLS from the ExPASY Server from the Geneva University Hospital and the University of Geneva (internet access: http://expasy.hcuge.ch/www/expasy-top.html).

Immunofluorescence

The strains were grown to an OD_{600} of ~1. To 25 ml of culture, 2.5 ml of 37% formaldehyde were added and incubation was continued for 1 h. The cells were put on ice for up to 90 min, harvested and resuspended in 100 mM Tris/HCl (pH 9.5, 24 °C), 10 mM DTT. The fixated cells were shaken for 8 min and centrifuged. The pellets were resuspended in 1 ml of buffer A [50 mM KP_i (pH 7.4, 24 °C), 1.2 M Sorbitol], washed, and resuspended in the same buffer containing 0.3 mg/ml Zymolyase 100T (Seigakaku Co.). Following incubation for 20 min at 30 °C, the cells were centrifuged, resuspended in buffer A and centrifuged twice (once at 24 °C, once at 4 °C). The pellet was resuspended in buffer A and the suspension was added to poly-L-lysine (Sigma)-treated coverslips and allowed to dry for five minutes. All subsequent steps were carried out in Buffer B (1 × PBS, 1% BSA, 0.5% Tween-20) at 24 °C. The coverslips were incubated for 20 min, washed four times for 5 min, and incubated upside down with 30 μl of buffer B containing the monoclonal mouse antibody A66 directed against Nop1p (dilution 1:30), affinity purified polyclonal antibodies directed against Lcp5p (dilution 1:100), or the mouse monoclonal antibody 12CA5 directed against the HA epitope (Boehringer Mannheim; dilution 1:10) for 1 h in a moist chamber. The coverslips were washed as above and overlayed with 200 μl of FITC-conjugated antibodies directed against rabbit IgG and Texas-Red-conjugated antibodies (Vector) directed against mouse IgG at a dilution of 1:250 for 1 h. The coverslips were washed as above, DAPI was added at a concentration of 0.5 μg/ml, and incubated for 5 min. The coverslips were washed twice as above. The cells were mounted in mowiol, followed by incubation for 10 min at 50 °C.

Microscopy

FITC, Texas Red, and DAPI were viewed by standard fluorescence microscopy through a FITC, TRITC, or UV filter, respectively, on a Nikon Microphot-FXA. FITC and Texas Red were viewed by confocal microscopy on a Noran Odyssey, equipped with an argon/krypton laser, with excitation wavelengths of 488 nm and 568.2 nm.

Immunoprecipitation

Total yeast extracts were prepared by glass bead lysis as described (Mitchell et al., 1996) from strain YTW12, expressing the HA-histidine-tagged Lcp5p. Lysis buffer consisted of 20 mM Tris pH 8.0 [24 °C], 150 mM KCl, 5 mM $MgCl_2$, 0.01% Triton X-100, 10 mM vanadyl-ribonucleoside complex (GIBCO), 2 mM phenylmethylsulfonylfluoride (Serva), and 1 mM DTT. The lysate was cleared by centrifugation for 10 min at 15,000 rpm. For immunoprecipitation, 50 μl of immune or preimmune serum were coupled to 80-μl-packed protein A sepharose (Pharmacia) in Ipp500 [10 mM Tris pH 8.0 (24 °C), 500 mM NaCl, 0.1% NaN_3, 0.1% NP40]. After overnight incubation at 4 °C, the pellets were washed in Ipp150 and 200 μl of yeast extract were added with an equal volume of Ipp150. The mixture was revolved for 2 h at 4–10 °C. After centrifugation the supernatant was discarded and the pellet was washed four times for 20 min at 4 °C with Ipp buffer of the indicated salt concentration. Proteins were digested with Proteinase K at 50 °C and RNAs were recovered by two PCI (phenol:chloroform:isoamylalcohol, 25:24:1) extractions. The RNA was ethanol precipitated, loaded on a denaturing 8% polyacrylamide gel, transferred to Hybond-N^+ filters (Amersham), and subjected to Northern hybridization with specific oligonucleotides (see RNA isolation, blotting and primer extension). For immunoprecipitation from strains expressing protein A-tagged fusion proteins, 20 μl of IgG Sepharose (Sigma) was equilibrated in Ipp150, then 100 μl of extract and 300 μl of Ipp150 were added and processed as above.

Genbank accession number

LPC5 has been assigned Genbank accession no. 603366.

ACKNOWLEDGMENTS

We thank F. Lacroute for contributing the yeast genomic library. We thank W. Keller for his support, and S. Barabino,

W. Keller, P. Linder, and M. Ohnacker for helpful suggestions and for reading the manuscript. We thank P.J. Preker, P. Linder, J. de la Cruz, D. Kressler, M. Beltrame, D. Tollervey and M. Caizergues-Ferrer for strains, materials and advice, and E. Hurt for the monoclonal antibody A66. This work was supported by grants to W. Keller from the Kantons of Basel, the Swiss National Science Foundation, and the European Union via the "Bundesamt für Bildung und Wissenschaft" (Bern). R.F.P. was supported by a grant to T. Bürglin from the Swiss National Science Foundation (No. 31-050839).

Received June 8, 1998; returned for revision June 30, 1998; revised manuscript returned July 27, 1998

REFERENCES

Allmang C, Henry Y, Morrissey JP, Wood H, Petfalski E, Tollervey D. 1996. Processing of the yeast pre-rRNA at sites A_2 and A_3 is linked. *RNA 2*:63–73.

Baudin-Baillieu A, Guillemet E, Cullin C, Lacroute F. 1997. Construction of a yeast strain deleted for the *TRP1* promoter and coding region that enhances the efficiency of the polymerase chain reaction-disruption method. *Yeast 13*:353–356.

Beltrame M, Tollervey D. 1995. Base pairing between U3 and the pre-ribosomal RNA is required for 18S rRNA synthesis. *EMBO J 14*:4350–4356.

Caponigro G, Parker R. 1995. Multiple functions for the poly(A)-binding protein in mRNA decapping and deadenylation in yeast. *Genes & Dev 9*:2421–2432.

Colgan DF, Manley JL. 1997. Mechanism and regulation of mRNA polyadenylation. *Genes & Dev 11*:2755–2766.

Collart MA, Oliviero S. 1994. Preparation of Yeast RNA. In: Ausubel FM, Brent R, Kingston RE, Moore DD, Seidman JG, Smith JA, Struhl K, eds. *Current Protocols in Molecular Biology.* New York: Current Protocols. pp 13.12.1–13.12.2.

Dingwall C, Laskey RA. 1991. Nuclear targeting sequences—a consensus? *Trends Biochem Sci 16*:478–481.

Doye V, Hurt E. 1997. From nucleoporins to nuclear pore complexes. *Curr Opin Cell Biol 9*:401–411.

Dunbar DA, Wormsley S, Agentis TM, Baserga SJ. 1997. Mpp10p, a U3 small nucleolar ribonucleoprotein component required for pre-18S rRNA processing in yeast. *Mol Cell Biol 17*:5803–5812.

Elela SA, Igel H, Ares M. 1996. RNase III cleaves eukaryotic preribosomal RNA at a U3 snoRNP-dependent site. *Cell 85*:115–124.

Eustice DC, Wilhelm JM. 1984a. Fidelity of the eucaryotic codon–anticodon interaction: Interference by aminoglycoside antibiotics. *Biochemistry 23*:1462–1467.

Eustice DC, Wilhelm JM. 1984b. Mechanisms of action of aminoglycoside antibiotics in eucaryotic protein synthesis. *Antimicrob Agents Chemother 26*:53–60.

Frank D, Patterson B, Guthrie C. 1992. Synthetic lethal mutations suggest interactions between U5 small nuclear RNA and four proteins required for the second step of splicing. *Mol Cell Biol 12*:5197–5205.

Gallie DR. 1991. The cap and poly(A) tail function synergistically to regulate mRNA translational efficiency. *Genes & Dev 5*:2108–2116.

Gallie DR, Tanguay R. 1994. Poly(A) binds to initiation factors and increases cap-dependent translation in vitro. *J Biol Chem 269*:17166–17173.

Ganot P, Caizergues-Ferrer M, Kiss T. 1997. The family of box ACA small nucleolar RNAs is defined by an evolutionarily conserved secondary structure and ubiquitous sequence elements essential for RNA accumulation. *Genes & Dev 11*:941–956.

Gietz D, St Jean A, Woods RA, Schiestl RH. 1992. Improved method for high efficiency transformation of intact yeast cells. *Nucleic Acids Res 20*:1425.

Guarente L. 1993. Synthetic enhancement in gene interaction: A genetic tool come of age. *Trends Genet 9*:362–366.

Guthrie C, Fink GR. 1991. *Guide to Yeast Genetics and Molecular Biology*. San Diego, California: Academic Press.

Haghighat A, Sonenberg N. 1997. eIF4G dramatically enhances the binding of eIF4E to the mRNA 5′-cap structure. *J Biol Chem 272*:21677–21680.

Hampsey M. 1997. A review of phenotypes in *Saccharomyces cerevisiae*. *Yeast 13*:1099–1133.

Harlow E, Lane D. 1988. *Antibodies: A laboratory manual*. Cold Spring Harbor, New York: Cold Spring Harbor Laboratory Press.

Huffacker TC, Hoyt MA, Botstein D. 1987. Genetic analysis of the yeast cytoskeleton. *Annu Rev Genet 21*:259–284.

Hughes JMX, Ares M. 1991. Depletion of U3 small nucleolar RNA inhibits cleavage in the 5′ external transcribed spacer of yeast pre-ribosomal RNA and impairs formation of 18S ribosomal RNA. *EMBO J 10*:4231–4239.

Jacobson A, Peltz SW. 1996. Interrelationships of the pathways of mRNA decay and translation in eukaryotic cells. *Annu Rev Biochem 65*:693–739.

Jansen R, Tollervey D, Hurt EC. 1993. A U3 snoRNP protein with homology to splicing factor PRP4 and Gβ domains is required for ribosomal RNA processing. *EMBO J 12*:2549–2558.

Jenny A, Minvielle-Sebastia L, Preker PJ, Keller W. 1996. Sequence similarity between the 73-kilodalton protein of mammalian CPSF and a subunit of yeast polyadenylation factor I. *Science 274*:1514–1517.

Keller W. 1995. No end yet to messenger RNA 3′ processing! *Cell 81*:829–832.

Keller W, Minvielle-Sebastia L. 1997. A comparison of mammalian and yeast pre-mRNA 3′-end processing. *Curr Opin Cell Biol 9*:329–336.

Kessler MM, Henry MF, Shen E, Zhao J, Gross S, Silver PA, Moore CL. 1997. Hrp1, a sequence-specific RNA-binding protein that shuttles between the nucleus and the cytoplasm, is required for mRNA 3′-end formation in yeast. *Genes & Dev 11*:2545–2556.

Kessler MM, Zhao J, Moore CL. 1996. Purification of the *Saccharomyces cerevisiae* cleavage/polyadenylation factor I. *J Biol Chem 271*:27167–27175.

Kressler D, de la Cruz J, Rojo M, Linder P. 1997. Fal1p is an essential DEAD-box protein involved in 40S-ribosomal-subunit biogenesis in *Saccharomyces cerevisiae*. *Mol Cell Biol 17*:7283–7294.

Lee W-C, Zabetakis D, Mélèse T. 1992. NSR1 is required for pre-rRNA processing and for the proper maintenance of steady-state levels of ribosomal subunits. *Mol Cell Biol 12*:3865–3871.

Li HV, Zagorski J, Fournier MJ. 1990. Depletion of U14 small nuclear RNA (snR128) disrupts production of 18S rRNA in *Saccharomyces cerevisiae*. *Mol Cell Biol 10*:1145–1152.

Lingner J. 1992. Biochemical and genetic analysis of poly(A) polymerase from *Saccharomyces cerevisiae*. Doctoral thesis. University of Basel, Basel, Switzerland.

Lupas A, Van Dyke M, Stock J. 1991. Predicting coiled coils from protein sequences. *Science 252*:1162–1164.

Lygerou Z, Allmang C, Tollervey D, Séraphin B. 1996. Accurate processing of a eukaryotic precursor ribosomal RNA by ribonuclease MRP in vitro. *Science 272*:268–270.

Manley JL, Takagaki Y. 1996. The end of the message—another link between yeast and mammals. *Science 274*:1481–1482.

Martens JA, Genereaux J, Saleh A, Brandl CJ. 1996. Transcriptional activation by yeast PDR1p is inhibited by its association with NGG1p/ADA3p. *J Biol Chem 271*:15884–15890.

Martin G, Keller W. 1996. Mutational analysis of mammalian poly(A) polymerase identifies a region for primer binding and a catalytic domain, homologous to the family X polymerases, and to other nucleotidyltransferases. *EMBO J 15*:2593–2603.

Mewes HW, Albermann K, Heumann K, Liebl S, Pfeiffer F. 1997. MIPS: A database for protein sequences, homology data and yeast genome information. *Nucleic Acids Res 25*:28–30.

Minvielle-Sebastia L, Preker PJ, Keller W. 1994. RNA14 and RNA15 proteins as components of a yeast pre-mRNA 3′-end processing factor. *Science 266*:1702–1705.

Minvielle-Sebastia L, Preker PJ, Wiederkehr T, Strahm Y, Keller W. 1997. The major yeast poly(A)-binding protein is associated with cleavage factor IA and functions in premessenger RNA 3′-end formation. *Proc Natl Acad Sci USA 94*:7897–7902.

Minvielle-Sebastia L, Windsor B, Bonneaud N, Lacroute F. 1991. Mutations in the yeast *RNA14* and *RNA15* genes result in an

abnormal mRNA decay rate; sequence analysis reveals an RNA-binding domain in the RNA15 protein. *Mol Cell Biol 11*:3075–3087.
Mitchell P, Petfalski E, Tollervey D. 1996. The 3′ end of yeast 5.8S rRNA is generated by an exonuclease processing mechanism. *Genes & Dev 10*:502–513.
Morrissey JP, Tollervey D. 1993. Yeast snR30 is a small nucleolar RNA required for 18S rRNA synthesis. *Mol Cell Biol 13*:2469–2477.
Nakai K, Kanehisa M. 1992. A knowledge base for predicting protein localization sites in eukaryotic cells. *Genomics 14*:897–911.
Palmer E, Wilhelm JM, Sherman F. 1979. Phenotypic suppression of nonsense mutants in yeast by aminoglycosidic antibiotics. *Nature 277*:148–150.
Pearson WR, Lipman DJ. 1988. Improved tools for biological sequence comparison. *Proc Natl Acad Sci USA 85*:2444–2448.
Preker PJ, Lingner J, Minvielle-Sebastia L, Keller W. 1995. The *FIP1* gene encodes a component of a yeast pre-mRNA polyadenylation factor that directly interacts with poly(A) polymerase. *Cell 81*:379–389.
Preker PJ, Ohnacker M, Minvielle-Sebastia L, Keller W. 1997. A multisubunit 3′ end processing factor from yeast containing poly(A) polymerase and homologues of the subunits of mammalian cleavage and polyadenylation specificity factor. *EMBO J 16*:4727–4737.
Proweller A, Butler JS. 1997. Ribosome concentration contributes to discrimination against poly(A)$^-$ mRNA during translation initiation in *Saccharomyces cerevisiae*. *J Biol Chem 272*:6004–6010.
Sachs AB, Davis RW. 1989. The poly(A) binding protein is required for poly(A) shortening and 60S ribosomal subunit-dependent translation initiation. *Cell 58*:857–867.
Sachs AB, Sarnow P, Hentze MW. 1997. Starting at the beginning, middle, and end: Translation initiation in eukaryotes. *Cell 89*:831–838.
Sachs A, Wahle E. 1993. Poly(A) tail metabolism and function in eucaryotes. *J Biol Chem 268*:22955–22958.
Sambrook J, Fritsch EF, Maniatis T. 1989. *Molecular Cloning: A Laboratory Manual*. Cold Spring Harbor, New York: Cold Spring Harbor Laboratory Press.
Schimmang T, Tollervey D, Kern H, Frank R, Hurt EC. 1989. A yeast nucleolar protein related to mammalian fibrillarin is associated with small nucleolar RNA and is essential for viability. *EMBO J 8*:4015–4024.
Singh A, Ursic D, Davies J. 1979. Phenotypic suppression and misreading in *Saccharomyces cerevisiae*. *Nature 277*:146–148.
Smith V, Chou KN, Lashkari D, Botstein D, Brown PO. 1996. Functional analysis of the genes of yeast chromosome V by genetic footprinting. *Science 274*:2069–2074.
Studier FW. 1991. Use of bacteriophage T7 lysozyme to improve an inducible T7 expression system. *J Mol Biol 219*:37–44.
Tarun SZ, Sachs AB. 1995. A common function for mRNA 5′ and 3′ ends in translation initiation in yeast. *Genes & Dev 9*:2997–3007.
Tarun SZ, Sachs AB. 1996. Association of the yeast poly(A) tail binding protein with translation initiation factor eIF-4G. *EMBO J 15*:7168–7177.
Tarun SZ, Wells SE, Deardorff JA, Sachs AB. 1997. Translation initiation factor eIF4G mediates in vitro poly(A) tail-dependent translation. *Proc Natl Acad Sci USA 94*:9046–9051.
Tollervey D. 1987. A yeast small nuclear RNA is required for normal processing of pre-ribosomal RNA. *EMBO J 6*:4169–4175.
Varshavsky A. 1996. The N-end rule: Functions, mysteries, uses. *Proc Natl Acad Sci USA 93*:12142–12149.
Venema J, Tollervey D. 1995. Processing of pre-ribosomal RNA in *Saccharomyces cerevisiae*. *Yeast 11*:1629–1650.
Venema J, Tollervey D. 1996. *RRP5* is required for formation of both 18S and 5.8S rRNA in yeast. *EMBO J 15*:5701–5714.
Wahle E, Keller W. 1996. The biochemistry of polyadenylation. *Trends Biochem Sci 21*:247–250.
Wilson R, Ainscough R, Anderson K, Baynes C, Berks M, Bonfield J, Burton J, Connell M, Copsey T, Cooper J, Coulson A, Craxton M, Dear S, Du Z, Durbin R, Favello A, Fulton L, Gardner A, Green P, Hawkins T, Hillier L, Jier M, Johnston L, Jones M, Kershaw J, Kirsten J, Laister N, Latreille P, Lightning J, Lloyd C, McMurray A, Mortimore B, O'Callaghan M, Parsons J, Percy C, Rifken L, Roopra A, Saunders D, Shownkeen R, Smaldon N, Smith A, Sonnhammer E, Staden R, Sulston J, Thierry-Mieg J, Thomas K, Vaudin M, Vaughan K, Waterston R, Watson A, Weinstock L, Wilkinson-Sproat J, Wohldman P. 1994. 2.2 Mb of contiguous nucleotide sequence from chromosome III of *C. elegans*. *Nature 368*:32–38.
Zhao J, Kessler MM, Moore CL. 1997. Cleavage factor II of *Saccharomyces cerevisiae* contains homologues to subunits of the mammalian cleavage/polyadenylation specificity factor and exhibits sequence-specific, ATP-dependent interaction with precursor RNA. *J Biol Chem 272*:10831–10838.